Chapter 5

Functionalized Polyvinylidene Fluoride Electrospun Nanofibers and Applications

Dinesh Lolla, Lin Pan, Harshal Gade and George G. Chase

Additional information is available at the end of the chapter

http://dx.doi.org/10.5772/intechopen.76261

Abstract

Electrospun polymeric nanofibers with flexible three-dimensional porous structures and high surface-to-volume ratio are potential resources for several novel applications in the fields of micro- and nanoscale filtration, water desalination, drug delivery, life sciences, catalysis, and energy harvesters. Functionalized polymeric fibers with enhanced molecular orientation, surface textural morphologies, and piezo-, pyro-, and ferroelectric properties are of technical and commercial interest around the world. Several emerging technologies including electrical polarization, vacuum plasma treatment, corona discharge, surface fluorination, and chemical treatments to functionalize the polyvinylidene fluoride nanofibers are discussed as potential applications of electroactive materials.

Keywords: electrospinning, polarization, aerosol filtration, salt absorption, catalysis

1. Polyvinylidene fluoride (PVDF) and its crystalline phases

Polyvinylidene fluoride (PVDF) is a semicrystalline, dielectric polymer with very high breakdown strength that offers long-duration surface charge retention, due to its unique dipole molecular structure with CH_2-CF_2 repeated monomer units [1]. PVDF is regarded as one of the most suitable polymeric materials to study polarizability in dielectric polymers. The dipole monomer structure of PVDF is favored in converting electromechanical coupling behavior with variance in thermomechanical processing. Although the piezoelectric coefficient of PVDF and its copolymers PVDF-HFP and PVDF-TrFE are less than piezoelectric ceramics like PBZ and $BaTiO_3$, their elasticity and mechanical stretchability make them more reliable materials for several emerging applications [2]. Moreover, PVDF exhibits higher piezoelectric response

voltage, good thermal stability, and chemical resistance suitable for sensors, aerosol filters, actuators, fuel cells, energy harvesters, and other applications [3–7].

Depending on the crystalline conformations, PVDF exhibits five different molecular morphologies labeled as α, β, γ, δ, and ε. The composition and distinctive character of individual and binary phases are studied using Fourier transform infrared spectrometry (FTIR) and X-ray diffractometry (XRD) analysis. The α-phase consists of a non-centrosymmetric crystal structure with CH_2-CF_2 dipoles oriented in the same direction and has an all-trans (TTTT) planar zigzag conformation [8]. The β-phase follows a trans-gauche-trans-gauche' (TGTG') atomic arrangement of a centrosymmetric unit cell. In this atomic configuration, the CH_2 dipoles are perpendicular to CF_2 repeat units, and this produces a permanent electric dipole perpendicular to the axis with corresponding strong and ferroelectric and piezoelectric charges. The γ-phase has T_3GT_3G' conformations where the CH_2-CF_2 dipoles are oriented parallel to each other to form a non-centrosymmetric polar crystal. In general, the γ- and δ-phases form as a result of high-pressure crystallization [8, 9], are not commonly observed in the electrospun fibers, and hence are not considered further here.

Phase transformations among the crystal orientations take place under various postprocessing such as heat treatment, uniaxial stretching, and electrical poling [9–11]. Phase transformational mechanisms caused by polarization are interpreted in terms of vibrational motions around the individual atomic bonds in the PVDF molecule. Two distinct motions, known as flip-flop (segmental) and inversion motions (macromolecular), were observed during transformation of phases in polarization treatments. The segmental flip-flop motions usually occur at about 150°C (the Curie temperature) and result in a gradual change in the molecular conformations. Higher temperatures above 170°C are usually needed to produce inversion motions but can be achieved near the Curie temperature by subjecting the PVDF fibers with simultaneous electromechanical effects. Heat treatment in the presence of high electric fields and elevated ambient pressures can produce transformations from α- to β-phase and β- to γ-phase (<280°C, <4000 atm). The reverse transformations from β- to α-phase and γ- to α-phase typically require higher temperature and pressure (>290°C, >4500 atm). The transformation from β- to α-phase has so far only been studied in the unoriented state. The γ-phase PVDF melting temperature is about 15°C higher than the α- and β-phase materials. In this chapter, we reported several phase conversion techniques with primary focus on enhancing the amount of β-phase in PVDF fibers using different functionalization routes.

2. Electrospinning

Electrospinning is well documented and is considered an easy laboratory method for producing submicron and nanofibers [12, 13]. Electrospun polymer fibers are widely used in filtration [14, 15], catalysis [16–22], biomedical materials [23–26], and electrolytes [7, 27].

The application of electrical forces to produce polymer filaments began in the early 1930s. A brief summary of the early electrospinning literature is provided by Huang et al. [28]. A highly cited reference describing the mechanisms of electrospinning is by Reneker et al. [29].

The electrospinning process is driven by the electrical forces on the surface or inside the polymer solution. The free charges (ions) inside the polymer solution move in response to the electrical field and transfer a force to the solution [29]. When the electrically induced forces exceed the surface tension force, a liquid jet is ejected from the surface [30].

A schematic diagram of a typical laboratory electrospinning setup is shown in **Figure 1**. The components are high-voltage power supply, a syringe pump that delivers polymer solution through a tube to a small diameter needle, and a grounded rotating drum collector surface. The high voltage creates the electrical charge in the solution, and a jet is driven by the potential between the needle and the collector. As the jet travels to the collector, the solvent evaporates, and the jet solidifies into small fibers that deposit on the collector surface.

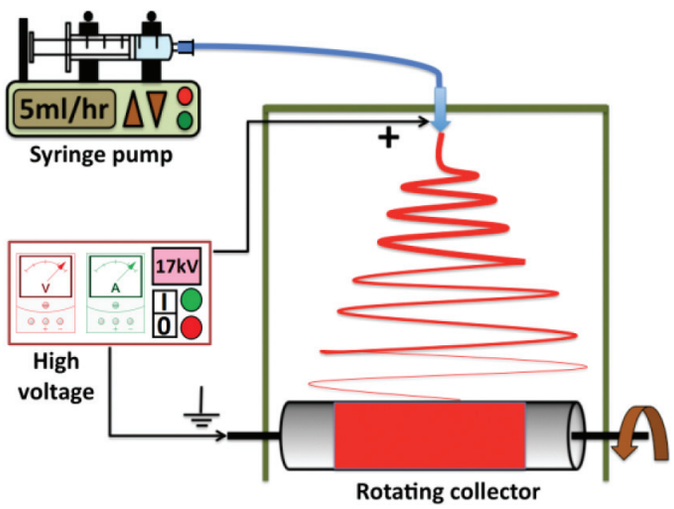

Figure 1. Schematic of a typical electrospinning setup used in this work.

MW	Conc. (%)	Solvent	Electrospun gap (volts)	Application	Ref.
107 K	20	DMF:DMA (1:1)	20 cm, 20 kV	Flat ribbons	[33]
	12–18	Ac:DMA (7:3)		Batteries	[31]
	25	DMA	15 cm, 10 kV	Electrolyte or separator	[37]
107 K		DMF:Ac (7:3) (v:v)	20 cm, 25 kV	Batteries	[34]
	15	DMF:Ac (2:8) (v:v)	8–15 kV	Metal cells	[38]
		DMF:Ac (6:4) (w:w)	12 cm, 25 kV 15 cm, 28 kV	Distillation	[39]
	20	DMF:Ac (7:3) (w:w)	15 cm, 25 kV	Separator	[40]
	14–24	DMF:Ac (3:7, 4:6, 5:5, 6:4, 7:3)	15 cm, 15–18 kV	Filtration	[41]
	16–20	DMS:Ac (1:1)	10–16 kV	Energy harvester	[42]
		DMF water (50:3) (w:w)	40 cm, 22.5 kV	Electrode	[43]

DMF, dimethylformamide; DMA, dimethylacetamide; DMS, dimethyl sulfoxide; Ac, acetone.

Table 1. Electrospinning of PVDF literature summary.

Many natural and synthetic polymers have been electrospun to produce fine fibers, such as polyacrylonitrile (PAN), polyvinyl alcohol (PVA), poly(methyl methacrylate) (PMMA), polyethylene oxide (PEO), polyethylene (PE), and polypropylene (PP) [31]. In comparison, PVDF has attracted much attention due to its properties and molecular structure. **Table 1** summarizes solution and spinning conditions for electrospinning PVDF fibers reported in literature. In addition, some researchers have modified the properties of the PVDF fiber mats by blending with other polymers [32]. As an example Gopalan et al. [34] mixed PVDF with varying amounts of PAN to fabricate fiber mats for use in lithium batteries. Ding and coworkers mixed PVDF with PMMA for same purpose, Guo et al. [35] prepared the PU/PVDF electrospun scaffolds for wound healing, and Dong et al. [36] electrospun PVDF/PTFE membranes for distillation.

3. Functionalization of polyvinylidene fluoride nanofibers

Properties of nanofibers, such as electrical, textural, optical, adhesive, and tensile strength, are highly dependent on the inherent polymeric properties and internal molecular structure. The chemical modification of polymer nanofibers introduces new characteristics to the materials that extend and enhance the scope of their industrial applications over several orders of magnitude. Hence, enhancement of molecular orientation of the PVDF nanofibers has attracted interest of the scientific community. A number of functionalization techniques are available in pilot and commercial scale operations. These functionalization processes can be economical, profitable, environmentally friendly, and long-term reliable [44, 45].

Fiber stretching during the electrospinning process causes dipoles to align perpendicular relative to each other [44]. Piezoresponse force microscopy (PFM) was used to analyze piezoelectric responses and ferroelectric domains in individual electrospun nanofibers with diameters 70, 170, and 400 nm [45]. The β-phase compositions of individual fibers were estimated in the 80–87% range using Beer-Lambert's law, confirming that fibers with smaller diameters experienced higher oriented conformational changes consistent with stronger elongational forces such as those produced with near-field electrospinning (NFES) due to short tip to collector distances.

Liu et al. [46] studied processing and solution conditions to obtain the highest β-content when PVDF was electrospun together with multiwalled carbon nanotubes (MWCNTs). Distinct oriented crystalline structures of the MWCNT/PVDF in aligned nanofibers were obtained. Due to the nucleation of highly oriented fibers and extended molecular crystallites at the interface, NFES techniques showed 28% increase in β-phase with 0.05% wt% of MWCNTs.

Served et al. [11] subjected a pre-stretched 100-μm-thick PVDF film containing exclusively α-phase with 5% head-to-head- and tail-to-tail-type (HHTT) defects to electrical poling at 80 and 170°C (T_m-178°C). Aluminum electrodes were placed on either side of the film, and a DC electric field of 1 MV/cm was used for charging. At 170°C the film changed from nonpolar α-phase to polar β-phase with TGTG molecular conformations. The β-phase polarized films showed a strong piezoelectric coefficient, d_{33} = 8.5pC/N, and was validated with XRD and FTIR analysis. Salimi et al. [47] analyzed β-content in compression-molded PVDF films made of two different grades of raw polymer (Kynar® 720, Hylar® MP10). A maximum of 74% β-phase was observed for films that were 38–40% crystalline at 90°C and stretched at a ratio

between 4.5 and 5. A similar study of nanoscale domain imaging and spatial distribution of d_{33} on single electrospun fibers concluded that the d_{33} distribution was more uniform along the length of the fibers compared to cross-sectional diameter [48].

Real-time piezoelectric responses were observed by manipulating the operational voltages of a PFM at a spring constant of 0.11 Nm^{-1}, with cantilever resonating frequency of 135 kHz and the amplitude changing stepwise from −30 to +30 V. The highest deflection in the piezoresponse hysteresis loop at 3.3 nm was observed at a V_{dc} of -30 V. XRD patterns decrypted using a curve deconvolution technique revealed 72.7% β-phase at plane (110,200) and 15.1% α-phase (202) and indicated voltages as much as ±30 V can cause significant effects on nanoscale β-phase nanocrystals. Nanodomains were distributed along to the fiber axis, and the β-phase orientation was investigated by TEM and XRD [48]. Furthermore, polymer composites can be polarized at low electric field strengths with addition of nanoparticle ferroelectric ceramics [49, 50].

Introduction of chemical functional groups into virgin PVDF polymer has resulted in novel functional characteristics [51, 52]. Several studies have reported the ability of modifying structural morphologies and analytical properties in electrospun PVDF nanofibers via plasma deposition of polymers under inert conditions. Molecular cross-linking on PVDF can be achieved through dehydrofluorination or by introducing functional comonomers during electrospinning [5, 8, 53].

The PVDF materials with modified properties are of significant practical interest. In filtration, for example, an exceptional particle capture efficiency of ≥99.999% was achieved by a hybrid monolithic electret aerogel composed of syndiotactic polystyrene (sPS)/PVDF [54], whereas 98.9% filtration efficiency was recorded with sPS monolithic aerogel comprised of similar solid content. In comparison, performance of cellulose acetate electrospun fibers with diameters in the range from 0.1 to 24 μm challenged with a solid brine aerosol (NaCl) and a liquid aerosol of (diethyl hexyl sebacate) showed a maximum efficiency of 70% and with the most penetrating particle size in the range of 40–270 nm [55].

4. Results and discussion

4.1. Electrospinning of PVDF fibers

Electrospinning solutions 10 wt% were prepared by dissolving Kynar® 761 grade resin (MW of about 550,000, melt viscosity of 35 kp, and a solution viscosity of 350cp at room temperature), PVDF powder (Arkema Inc., USA) in cosolvents N-N-dimethylformamide (DMF), and acetone (Sigma-Aldrich, USA). The solutions were electrospun under the conditions reported in **Table 2**.

Mats of 20 g/m^2 basis weight were preheated in an oven at 70°C for 4 hrs before any analysis. Fiber morphologies were analyzed under a scanning electron microscope. Smooth and consistent fibers were observed as shown in **Figure 2**. A maximum of 57.7% β-content in the fibers was observed. SEM images occasionally showed branched fibers. Branched fibers were formed because of "static equilibrium undulations under the combined effect of the electric Maxwell stresses and surface tension as the electrical stresses are increased" [56].

Conc. PVDF (wt%)	DMF: acetone (w: w)	Gap distance (cm)	Voltage (kV)	Flow rate (mL/h)	Collector rotation (RPM)	Avg. fiber dia. (nm)	Standard deviation (nm)
10	1:1	20	17	5	100	196	54

Table 2. Electrospinning conditions and average PVDF fiber diameter.

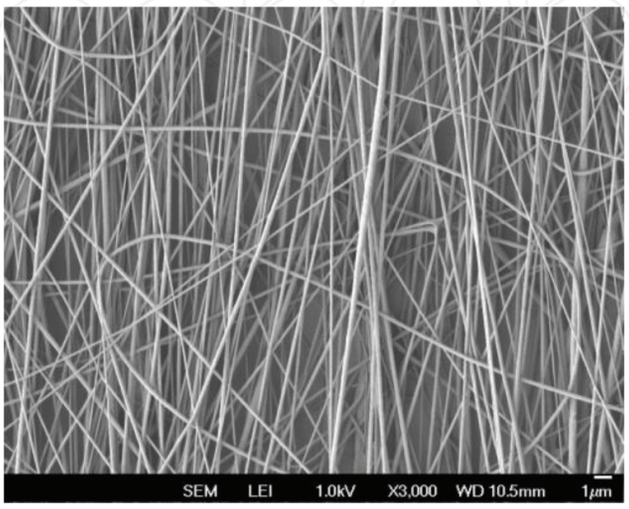

Figure 2. SEM image of 10 wt% PVDF, 1:1 DMF/acetone electrospun fibers.

4.2. Atomic resolution electron microscopy of PVDF nanofibers

A segment of 8X5nm PVDF fiber was studied under an aberration-corrected electron microscope with highly controlled electron beam shown in **Figure 3**. The images revealed the paths of individual monomers aligned in the direction of fiber axis as shown in **Figure 3A**. CF_2 bonds appeared as brighter dots compared to other bonds as gray and black dots. The raw TEM micrograph was converted into a Fourier transform image to reduce the electron noise and reverted as an RGB image to enhance the features. Paths of CF_2 molecules from end to end are clearly seen in the enhanced RBG image in **Figure 3B**. The calculated distance between the centers of two adjacent bright dots in **Figure 3B** is about 0.25 nm which is consistent with molecular dynamic simulation of the theoretical distance between fluorine atoms in the β-phase crystallographic structure of the PVDF [1] in **Figure 3C**.

4.3. Functionalization of PVDF nanofibers by electrical polarization

Lolla et al. [7] describe a thermal-stretch-electric field polarization treatment of PVDF nanofibers to fabricate polarized PVDF fiber mats. Simultaneous thermal and electrical treatments caused substantial changes in surface textural morphology. These surface morphological changes are obvious when as-spun fibers shown in **Figure 4A** are compared to the thermal-electrically treated fibers in **Figure 4B**.

http://dx.doi.org/10.5772/intechopen.76261

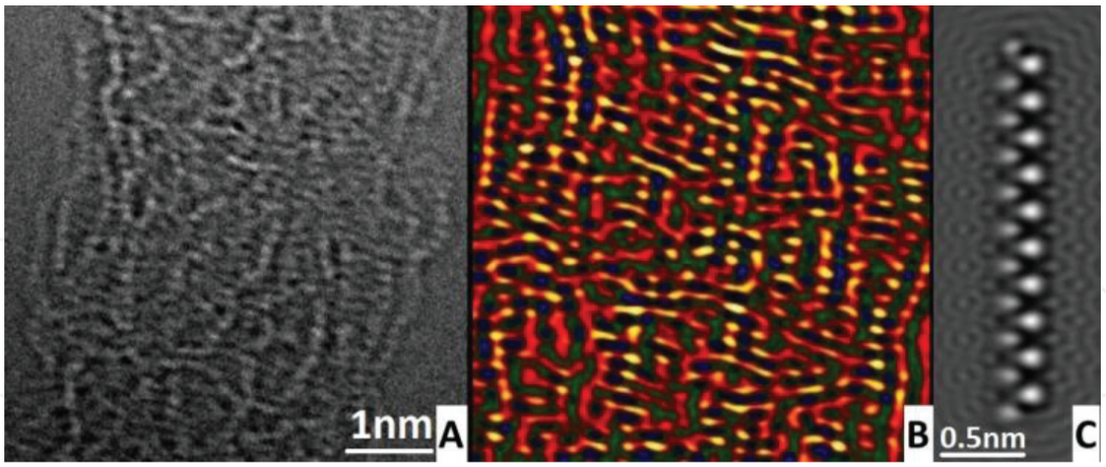

Figure 3. (A) Raw high magnification TEM image of PVDF nanofiber, (B) Fourier transform of raw image, and (C) molecular dynamic simulation of PVDF molecule.

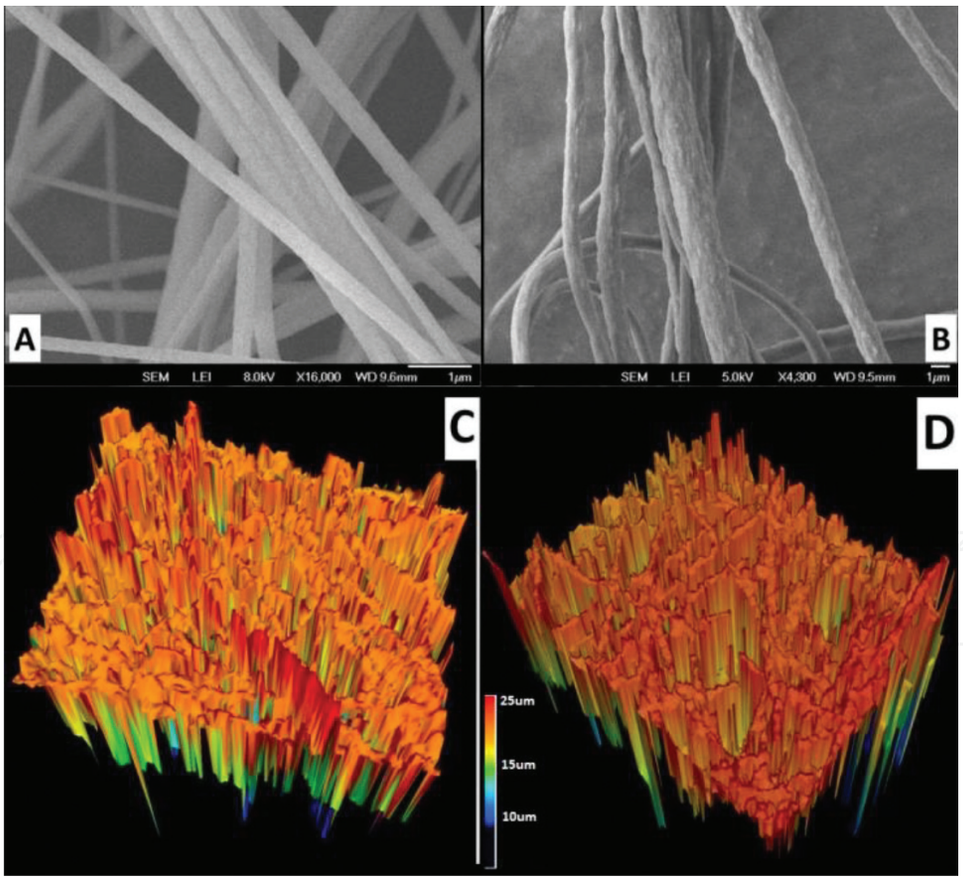

Figure 4. Surface morphology analysis using high magnification SEM (images A and B) and laser microscopy (images C and D). The fiber samples in images A and C were as-spun fibers, and the images B and D were thermal-electric treated polarized PVDF nanofibers.

Surface modifications were found to have a remarkable effect during liquid–liquid filtration applications compared to aerosol filtration as the interfacial strength between liquid droplets is much higher in polarized fiber mats compared to relatively smooth fibers. Kinetic energy generated by electron collision during charge migration is suspected to be the primary reason for surface irregularities. SEM analysis provided only 2D visual conformation of polarization-associated surface modifications. A complete three-dimensional analysis was done to obtain precise increase in roughness due to electron interaction. Lasers were projected in z-direction with the fibers across a 20×30×25μm sample, and few thousands of data points were gathered from hundreds of fibers to make the analysis. All the fiber samples were highly irregular with several mounds, hills, and valley-like structures as shown in **Figure 4C** and **D**. Unlike the 2D SEM images, the detailed layer-by-layer fiber interactions were seen, and paths of fiber conglutination or fiber cross-linking were more accurately captured in several directions using laser projections.

2D images of laser intensities were obtained in parallel with three-dimensional images, and an empirical analysis was conducted to estimate the changes in surface morphology. As-spun fibers and thermal-electric treated fibers are shown in **Figure 5A** and **B**. The data analysis was conducted on the circular areas highlighted in the images. The radii of the circles in both images were 40 μm. The average intensities of as-spun fibers from peak to valley detection were mapped as shown in **Figure 5C** represented by the blue line, which gave us a mean surface roughness of R_{ms} = 7.86 ± 4.73 nm. Similar calculations were also performed on the thermal-electric treated fibers, and the mean surface roughness R_{ms} of 16.86 ± 6.68 nm was

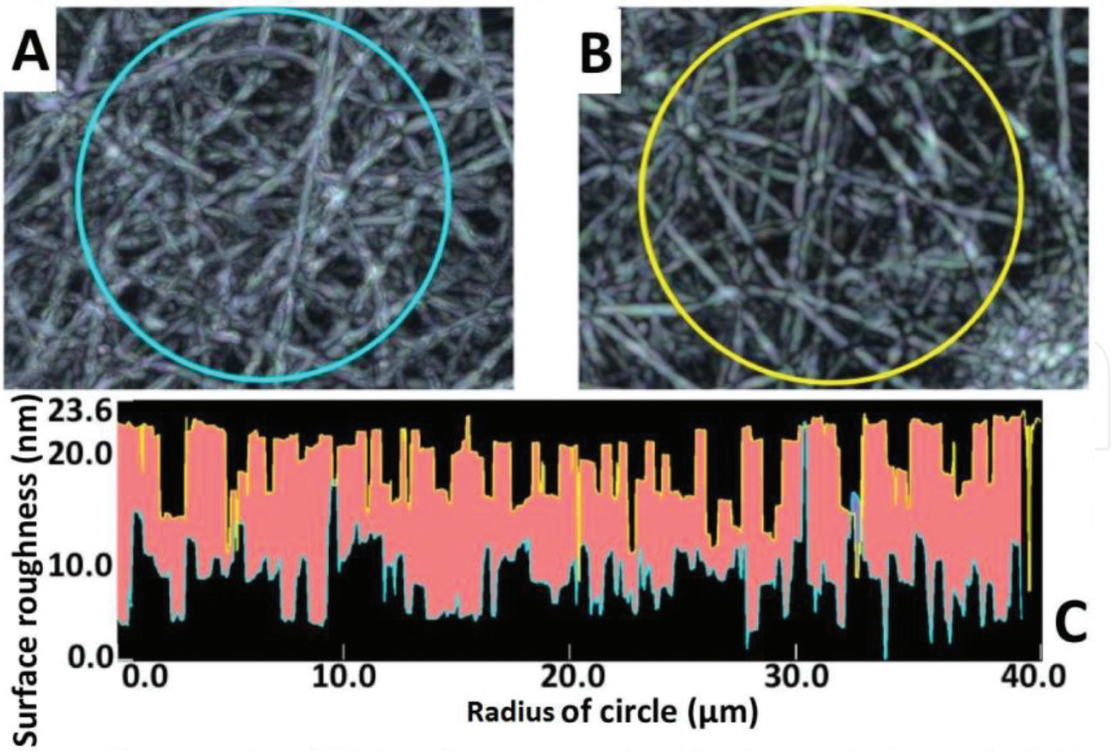

Figure 5. Comparison of surface roughness (A) as spun (B) polarized fibers (C) graphical overlay of surface roughness distribution.

determined which proves a substantial rise in surface roughness. Average values of roughness averaged over the length of the circumference of circles of varying radius from 0 to 40 μm was used to make a comparison between as-spun and polarized fibers.

4.3.1. Nanoscale aerosol particle filtration

Functionalized electrospun fibers are of great interest in aerosol filtration [57]. Fiber mats were subjected to aerosols of 10–250 nm diameter NaCl particles using a TSI-automated filter tester (TSI 8130). Each test was conducted for a duration of 10 s at 10 l/min volumetric flowrate. Three individual samples were consecutively tested 30 times with 30 days between tests to generate a particle capture v/s pressure buildup profile. For thermal-electrically treated polarized fiber mats, the first tests were performed within 24 h of polarization. Both the as-spun and polarized samples showed very distinct and diverse capture trends as apparent from **Figure 6A** and **B**. Further research with these materials and with theoretical predictions is needed to explore and understand the shelf life of the filter media in association with net charge. The polarized fibers did not exhibit cake formation, even for the smallest fiber diameters, and had much smaller pressure drop compared to the as-spun fibers. Almost all of the aerosol particles were evenly distributed among individual fibers in the polarized mat as compared to the agglomerates observed in the mat of as-spun fibers.

The plots in **Figure 7A** show the filter efficiency and pressure drop as a function of the number of tests. Effectively, the plot shows the filter performance over time as it was affected by loading of particles and by charge dissipation (if dissipation occurs) over an extended time. Both the as-spun and polarized filters recorded similar efficiencies of 94.63 ± 012 and 94.96 ± 0.46 during the first experimental run with pressure drops of 56 ± 1.63 and 49.66 ± 1.69 mmH_2O, respectively. Pressure drops across the media are in good agreement with the air permeability as shown in **Figure 7B**.

The Frasier air permeabilities of the fiber mats were tested at two different test pressures at 125 and 2000 kPa. The Darcy law permeability has units of area, whereas the Frazier permeability is reported as volumetric flow rate (cfm = cubic feet per minute). The Darcy permeability can be calculated, but for the purposes here, the relative magnitudes of the two flow rates are the relevant data. The plot in **Figure 7B** shows that the relative flow rates of the polarized mats

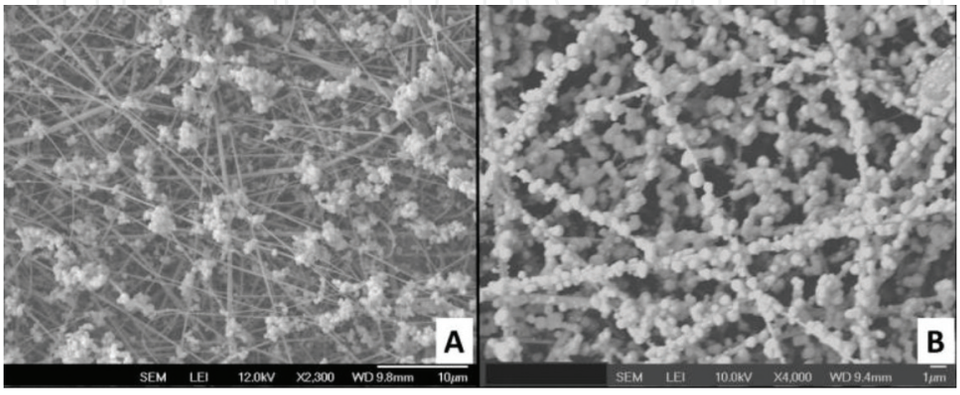

Figure 6. Brine (NaCl) aerosol captures on (A) as-spun and (B) polarized PVDF filter media.

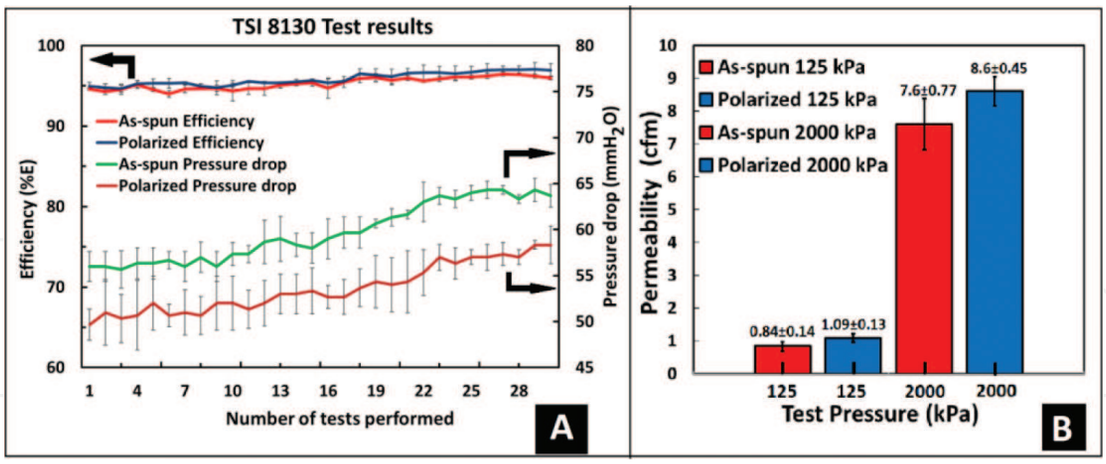

Figure 7. Aerosol penetration testing and Frazier permeability (i.e., flow rate at applied pressure) of as-spun and polarized fibers.

were about 17% greater than the flow rates of the as-spun mats, which corresponds to about 17% greater Darcy permeabilities in the polarized mats.

The pressure of 2000 psi is 16 times the pressure drop of 125. If the Darcy permeability was constant, then one would expect the flow rate to increase by a factor of 16 as the pressure increased. The data show that an increase of flow rate was only on order of a factor of 8 times. This indicates that as the flow rate increased the fiber mat structures may have deformed and caused a higher resistance to flow. This topic needs future investigation.

Inspection of SEM images showed attraction between fibers in the polarized mat that caused the fibers to rearrange relative to each other in the fiber mat which resulted in larger pores than the pores in the as-spun mat and is a likely cause of the increase in permeability of the polarized mats. At the end of the 30 filtration experiments, a slight increase in efficiency due to particle accumulation was observed in both the samples. The as-spun fiber mats had a maximum efficiency of 96% at 64 mmH_2O pressure drop, and the polarized fibers had a maximum efficiency of 97% pressure drop of 58 mmH_2O. Because both efficiencies were very similar, the significant advantage of the polarized mats was the reduced pressure drop.

4.3.2. Functionalized PVDF nanofibers in water desalination and purification

Population growth, industrialization, rise in living standards, and rapid climate changes have an increased demand for water significantly [58]. Water desalination and purification are a possible solution for providing fresh drinking water to the world especially in drought-prone regions [59]. Researchers have developed several treatment processes such as reverse osmosis (RO), nanofiltration (NF), ultrafiltration (UF), and thermal methods such as membrane distillation to improve water quality and supply. These techniques are energy intensive and have high operating and maintenance costs which make it difficult for developing countries to implement [59]. Membrane distillation finds limited application due to lack of a variety of membranes that can produce stable and high flux for a long time [60].

Industrial effluents contain a wide range of hazardous and toxic substances including heavy metal ions (Cd^{2+}, Pb^{2+}, Hg^{2+}, Zn^{2+}, etc.), organic acids, nitro compounds, hydrocarbons, sulfides (S^{2-}), sulfites (SO_3^{2-}), and sugars. Heavy metal pollution can cause serious environmental and health problems to humans [61]. Various methods used for heavy metal removal include ion exchange, electrodialysis, chemical precipitation, and solid-phase extraction [62–64]. Materials such as nanoparticles, polymers, and organic and inorganic compounds have been employed in the form of thin films, membranes, or powder for water treatment [65]. Apart from these, using a nano-adsorbent for heavy metal removal via adsorption mechanisms is a growing area of research because of its large surface area and mechanical strength [66]. However, regeneration of nano-adsorbents after water treatment is a challenge as adsorption activity decreases with time due to agglomeration. To overcome this challenge, nano-adsorbents can be modified using functionalization techniques [67].

Blending PVDF with inorganic materials such as ZrO_2 [68], ZnO [69], Al_2O_3 [70], Fe_3O_4 [71], CdS [72], SiO_2 [73], and TiO_2 [74] to increase adsorption capacity can help in heavy metal ion removal. This research area is of growing interest. For example, Zhang et al. [75] used ZnO-hybridized (PVDF/ZnO) membranes for adsorption and desorption studies of Cu^{2+} ions.

Zhao et al. [76] studied melamine-diethylenetriaminepentaacetic acid/polyvinylidene fluoride (MA-DTPA/PVDF)-chelating membranes bearing polyaminecarboxylate groups for removal of Ni^{2+} ions from wastewater. Salehi et al. [77] studied adsorption of Ni^{2+} and Cd^{2+} ions using 8-hydroxyquinoline ligand-immobilized PVDF membrane.

Na^+, Cl^-, and SO_4^{2-} ions are present in significant concentrations in typical seawater and brackish waters [78]. Most of the feeds subjected to desalination processes have sodium chloride (NaCl) or sulfates of Ca and Mg.

Table 3 is a brief literature summary of the electrospun fiber membranes applied to desalination performance. PVDF is generally applied in the as-spun condition. Few data are available on performance of functionalized PVDF for this application.

4.3.3. Membrane and polymer nanofiber catalyst

Membrane-based separations and heterogeneous chemical reactions are often treated as independent processes. The advantages of combining the two operations have drawn attention to membrane reactors that combine reaction and separation in a single-unit operation [86]. The properties of PVDF fiber mats naturally lend themselves to use as membrane reactors. The PVDF fiber mats have strength, can be embedded or coated with catalyst particles, have thermal stability over a useful temperature range, are inert to many chemical environments, can be superhydrophobic, and thus provide a barrier to aqueous solutions while being porous to gases.

Catalytic membrane reactors can be fabricated of materials that can selectively remove the reaction products from the reactor to increase the product yield. Membranes as catalyst support structures can provide relatively large surface areas, especially when the electrospun fibers are very small, for supporting catalyst particles [87].

Electrospun layer	Second layer/ treatment	Solute	Method	Flux (L/m^2/h)	Rejection	Ref.
PVDF	Polyamides	$MgSO_4$	TFNC by interfacial	0.66	75.7	[79]
		NaCl		0.66	70.2	
PVDF	n.a.	6%wt NaCl	AGMD	11–12 kg/m^2 h	n.a.	[80]
PVDF, clay nanocomposites	n.a.	NaCl	DCMD	n.a.	98.27 99.95	[81]
PET/PS	Polyamides	NaCl	Interfacial	1.13 L m^{-2}h^{-1}bar^{-1}	n.a.	[82]
PVDF-HFP (hot pressed)	Hot pressed	NaCl	DCMD	20–22 L h^{-1} min^{-2}	98	[83]
PAN	Polyamides	$MgSO_4$	TFNC interfacial	81	84.5	[84]
PVDF-PTFE	Microporous PTFE	NaCl	VMD	18.5 kg/m^2 h	99.9	[36]
PVDF-co-HFP	PAN microfibers	35 g/L NaCl	DCMD	45–30 L h^{-1} min^{-2}	n.a.	[85]
Intrinsically modified PVDF	Ag nanoparticles	3.5 wt% NaCl	DCMD	31.8 L h^{-1} min^{-2}	n.a.	[60]

DCMD, direct contact membrane distillation; AGMD, air gap membrane distillation; TFNC, thin-film nanocomposite; VMD, vacuum membrane distillation.

Table 3. Performance of various electrospun polymeric nanofibers used in water desalination techniques in pristine form or in modified conditions.

Inorganic membranes can provide high-temperature durability and easy loading of catalyst [88]. However, polymer membranes have the advantages including flexibility, easy for recycling [89], and affinity for reagents [90].

Electrospun fiber membranes have been studied for their physical and chemical properties, mechanical performance [28], large surface areas, and high porosities [19]. Pinto et al. [16] studied polystyrene electrospun fibers for catalysts and nanopore filter applications. Electrospun PVDF nanofibers were studied by Li et al. [19] for immobilizing $CoCl_2$ catalyst for hydrolysis of $NaBH_4$. The high thermal stability, moduli, and mechanical strength of the PVDF fibers showed excellent catalytic activity and recycling stability.

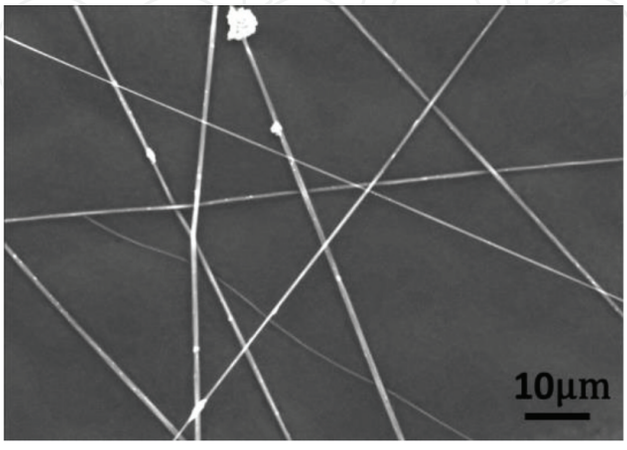

Figure 8. SEM image of electrospun PVDF+Pd black fibers.

In the work here, palladium (Pd) immobilized on PVDF electrospun fiber mats was investigated for catalytic hydrogenation of phenol to cyclohexanone. The one-step reaction can directly hydrogenate phenol into cyclohexanone, and the hydrogenation can be conducted either in liquid or gas phase. A two-step reaction is also possible in which phenol is first hydrogenated to cyclohexanol and then dehydrogenated to cyclohexanone [91]. PVDF and PVDF-HFP electrospun fiber mats are hydrophobic, resist the flow of water through the membrane, and provide a barrier between phenol water solution and hydrogen gas. **Figure 8** has SEM images of PVDF+5% Pd black samples.

Figure 9 shows EDX images of PVDF fibers with Pd black particles. The elemental Pd (appears in green color) on fibers. The fibers appear red due to elemental fluoride. Similar results were obtained for PVDF-HFP electrospun fiber mats.

Batch tests were conducted with Pd supported on PVDF-HFP fibers with 5, 10, and 15 wt% of Pd black. The average fiber diameter was 357 nm. The fiber mats were immersed in 75 mL of phenol/water solution (20 g/L) at 80°C under mild stirring and exposed to H_2 gas bubbles.

Reaction sample concentrations were measured by GC. The conversion and selectivity were calculated based on concentration changes. The reaction conversion increased with the concentration of Pd black and reached 98% conversion after 7 hours. The selectivity for cyclohexanone was about 97% for all of the fiber samples.

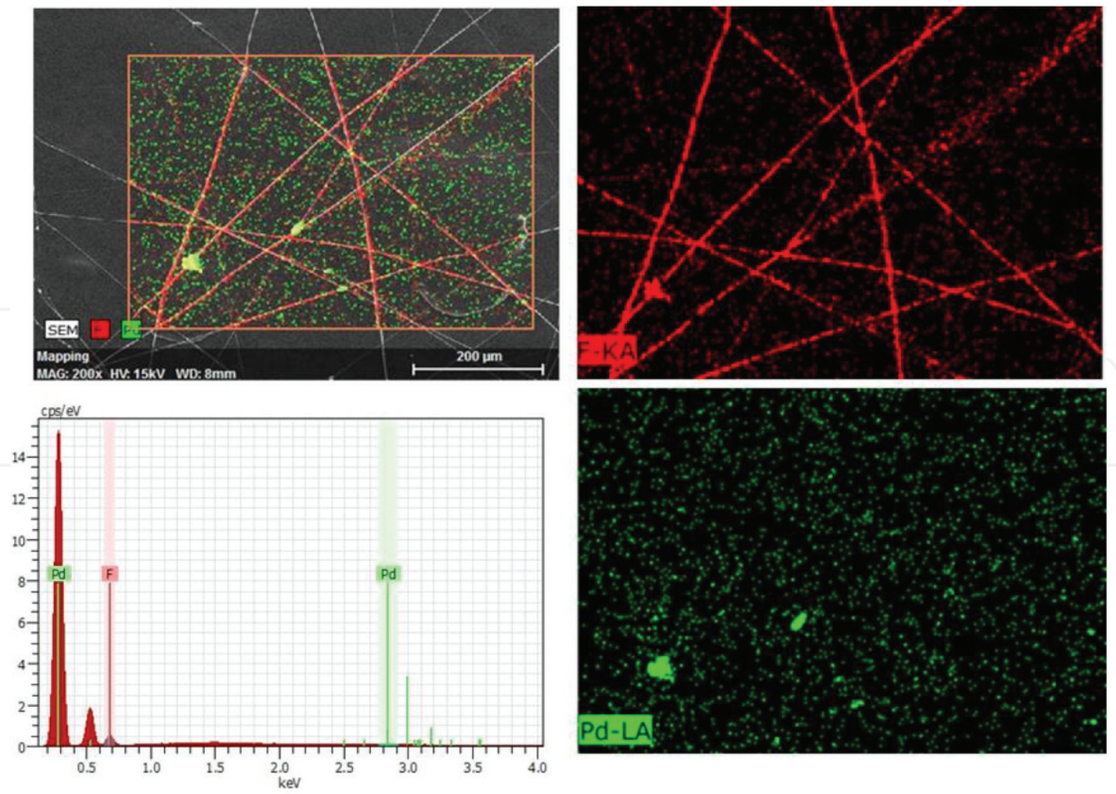

Figure 9. Energy dispersity X-ray (EDX) images of electrospun PVDF +5 wt% Pd black fibers.

5. Conclusion

In this work, PVDF and related copolymer mixtures are discussed. PVDF has unique properties due to its CH_2-CF_2 repeated monomer units that make it a material of recent scientific interest. Several applications of the electrospun PVDF polymer were reviewed. The PVDF molecule can be polarized. The polarized fiber mats were tested as aerosol filter media. SEM images showed remarkably different performances due to changes in particle capture mechanisms.

The PVDF membranes have potential applications for water treatment, first as a filter but second as a desalination membrane. The inherent dipole charges due to the CH_2-CF_2 repeated monomer units may be useful for separating salt ions from water. The last topic discussed is the use of PVDF and related copolymers as catalyst supports. As an example, experimental data for hydrogenation of phenol is presented. The limited amount of experimental data available showed that the PVDF membranes can be used for these applications. Further work is needed on these topics to determine the full potential of PVDF and related copolymer electrospun fiber mats.

Author details

Dinesh Lolla[1], Lin Pan[2]*, Harshal Gade[2] and George G. Chase[2]

*Address all correspondence to: lp57@zips.uakron.edu

1 Bioscience and Water Filtration Division, Parker-Hannifin Corporation, Oxnard, CA, United States

2 Department of Chemical and Biomolecular Engineering, The University of Akron, Akron, OH, United States

References

[1] Lolla D, Gorse J, Kisielowski C, Miao J, Taylor PL, Chase GG, et al. Polyvinylidene fluoride molecules in nanofibers, imaged at atomic scale by aberration corrected electron microscopy. Nanoscale. 2016;**8**:120-128. DOI: 10.1039/C5NR01619C

[2] Kilic A, Shim E, Yeom BY, Pourdeyhimi B. Improving electret properties of PP filaments with barium titanate. Journal of Electrostatics. 2013;**71**:41-47. DOI: 10.1016/j.elstat.2012.11.005

[3] Damaraju SM, Wu S, Jaffe M, Arinzeh TL. Structural changes in PVDF fibers due to electrospinning and its effect on biological function. Biomedical Materials. 2013;**8**:045007. DOI: 10.1088/1748-6041/8/4/045007

[4] Gaur A, Kumar C, Shukla R, Maiti P. Induced piezoelectricity in poly(vinylidene fluoride) hybrid as efficient energy harvester. ChemistrySelect. 2017;**2**:8278-8287. DOI: 10.1002/slct.201701780

[5] Li H-Y, Liu Y-L. Nafion-functionalized electrospun poly (vinylidene fluoride)(PVDF) nanofibers for high performance proton exchange membranes in fuel cells. Journal of Materials Chemistry A. 2014;**2**:3783-3793. DOI: 10.1039/C3TA14264G

[6] Liu S, Kim JT, Kim S. Effect of polymer surface modification on polymer–protein interaction via hydrophilic polymer grafting. Journal of Food Science. 2008;**73**. DOI: 10.1111/j.1750-3841.2008.00699.x

[7] Lolla D, Lolla M, Abutaleb A, Shin HU, Reneker DH, Chase GG. Fabrication, polarization of electrospun polyvinylidene fluoride electret fibers and effect on capturing nanoscale solid aerosols. Materials. 2016;**9**:671. DOI: 10.3390/ma9080671

[8] Sessler G. Piezoelectricity in polyvinylidenefluoride. The Journal of the Acoustical Society of America. 1981;**70**:1596-1608. DOI: 10.1121/1.387225

[9] Baniasadi M, Xu Z, Cai J, Daryadel S, Quevedo-Lopez M, Naraghi M, et al. Correlation of annealing temperature, morphology, and electro-mechanical properties of electrospun piezoelectric nanofibers. Polymer. 2017;**127**:192-202. DOI: 10.1016/j.polymer.2017.08.053

[10] Tashiro K, Takano K, Kobayashi M, Chatani Y, Tadokoro H. Phase transition at a temperature immediately below the melting point of poly (vinylidene fluoride) from I: A proposition for the ferroelectric curie point. Polymer. 1983;**24**:199-204. DOI: 10.1016/0032-3861(83)90133-7

[11] Servet B, Rault J. Polymorphism of poly (vinylidene fluoride) induced by poling and annealing. Journal de Physique. 1979;**40**:1145-1148. DOI: 10.1051/jphys:0197900400120114500

[12] Chase G, Zhang X. Solid aerosol filtration by electrospun poly vinyl pyrrolidone fiber mats and dependence on pore size. Journal of Textile Engineering and Fashion Technology. 2017;**1**. DOI: 10.15406/jteft.2017.01.00030

[13] Zhang X, Chase GG. Electrospun elastic acrylonitrile butadiene copolymer fibers. Polymer. 2016;**97**:440-448. DOI: 10.1016/j.polymer.2016.05.063

[14] Shin C, Chase GG, Reneker DH. Recycled expanded polystyrene nanofibers applied in filter media. Colloids and Surfaces A: Physicochemical and Engineering Aspects. 2005;**262**:211-215. DOI: 10.1016/j.colsurfa.2005.04.034

[15] Viswanadam G, Chase GG. Water–diesel secondary dispersion separation using superhydrophobic tubes of nanofibers. Separation and Purification Technology. 2013;**104**:81-88. DOI: 10.1016/j.seppur.2012.11.020

[16] Torres B, editor. Ultrafine fibers of polystyrene dissolved in tetrahydrofuran prepared using the electrospinning method. In: Proceeding of the National Conference on Undergraduate Research; 2001 15-17 March 2001; Kentucky

[17] Cheng HH, Chen F, Yu J, Guo ZX. Gold-nanoparticle-decorated thermoplastic polyurethane electrospun fibers prepared through a chitosan linkage for catalytic applications. Journal of Applied Polymer Science. 2017;**134**. DOI: 10.1002/app.44336

[18] Shi W, Li H, Zhou R, Qin X, Zhang H, Su Y, et al. Preparation and characterization of phosphotungstic acid/PVA nanofiber composite catalytic membranes via electrospinning for biodiesel production. Fuel. 2016;**180**:759-766. DOI: 10.1016/j.fuel.2016.04.066

[19] Li Q, Chen Y, Lee DJ, Li F, Kim H. Preparation of Y-zeolite/$CoCl_2$ doped PVDF composite nanofiber and its application in hydrogen production. Energy. 2012;**38**:144-150. DOI: 10.1016/j.energy.2011.12.021

[20] Shin HU, Lolla D, Nikolov Z, Chase GG. Pd–Au nanoparticles supported by TiO_2 fibers for catalytic NO decomposition by CO. Journal of Industrial and Engineering Chemistry. 2016;**33**:91-98. DOI: 10.1016/j.jiec.2015.09.020

[21] Shin HU, Abutaleb A, Lolla D, Chase GG. Effect of calcination temperature on NO–CO decomposition by Pd catalyst nanoparticles supported on alumina nanofibers. Fibers. 2017;**5**:22. DOI: 10.3390/fib5020022

[22] Abutaleb A, Lolla D, Aljuhani A, Shin HU, Rajala JW, Chase GG. Effects of surfactants on the morphology and properties of electrospun polyetherimide fibers. Fibers. 2017;**5**:33. DOI: 10.3390/fib5030033

[23] Kenawy E-R, Bowlin GL, Mansfield K, Layman J, Simpson DG, Sanders EH, et al. Release of tetracycline hydrochloride from electrospun poly (ethylene-co-vinylacetate), poly (lactic acid), and a blend. Journal of Controlled Release. 2002;**81**:57-64. DOI: 10.1016/S0168-3659(02)00041-X

[24] Matthews JA, Wnek GE, Simpson DG, Bowlin GL. Electrospinning of collagen nanofibers. Biomacromolecules. 2002;**3**:232-238. DOI: 10.1021/bm015533u

[25] Kenawy E-R, Layman JM, Watkins JR, Bowlin GL, Matthews JA, Simpson DG, et al. Electrospinning of poly (ethylene-co-vinyl alcohol) fibers. Biomaterials. 2003;**24**:907-913. DOI: 10.1016/S0142-9612(02)00422-2

[26] Rajala JW, Shin HU, Lolla D, Chase GG. Core–shell electrospun hollow aluminum oxide ceramic fibers. Fibers. 2015;**3**:450-462. DOI: 10.3390/fib3040450

[27] Choi SW, Kim JR, Ahn YR, Jo SM, Cairns EJ. Characterization of electrospun PVDF fiber-based polymer electrolytes. Chemistry of Materials. 2007;**19**:104-115. DOI: 10.1021/cm060223+

[28] Huang Z-M, Zhang Y-Z, Kotaki M, Ramakrishna S. A review on polymer nanofibers by electrospinning and their applications in nanocomposites. Composites Science and Technology. 2003;**63**:2223-2253. DOI: 10.1016/S0266-3538(03)00178-7

[29] Reneker DH, Yarin AL, Fong H, Koombhongse S. Bending instability of electrically charged liquid jets of polymer solutions in electrospinning. Journal of Applied Physics. 2000;**87**:4531. DOI: 10.1063/1.373532

[30] Katta P, Alessandro M, Ramsier R, Chase G. Continuous electrospinning of aligned polymer nanofibers onto a wire drum collector. Nano Letters. 2004;**4**:2215-2218. DOI: 10.1021/nl0486158

[31] Kim JR, Choi SW, Jo SM, Lee WS, Kim BC. Electrospun PVdF-based fibrous polymer electrolytes for lithium ion polymer batteries. Electrochimica Acta. 2004;**50**:69-75. DOI: 10.1016/j.electacta.2004.07.014

[32] Kang G-D, Cao Y-M. Application and modification of poly (vinylidene fluoride)(PVDF) membranes—A review. Journal of Membrane Science. 2014;**463**:145-165. DOI: 10.1016/j.memsci.2014.03.055

[33] Koombhongse S, Liu W, Reneker DH. Flat polymer ribbons and other shapes by electrospinning. Journal of Polymer Science Part B: Polymer Physics. 2001;**39**:2598-2606. DOI: 10.1002/polb.10015

[34] Gopalan AI, Santhosh P, Manesh KM, Nho JH, Kim SH, Hwang C-G, et al. Development of electrospun PVdF–PAN membrane-based polymer electrolytes for lithium batteries. Journal of Membrane Science. 2008;**325**:683-690. DOI: 10.1016/j.memsci.2008.08.047

[35] Guo H-F, Li Z-S, Dong S-W, Chen W-J, Deng L, Wang Y-F, et al. Piezoelectric PU/PVDF electrospun scaffolds for wound healing applications. Colloids and Surfaces B: Biointerfaces. 2012;**96**:29-36. DOI: 10.1016/j.colsurfb.2012.03.014

[36] Dong Z-Q, Ma X-h, Xu Z-L, You W-T, Li F-b. Superhydrophobic PVDF–PTFE electrospun nanofibrous membranes for desalination by vacuum membrane distillation. Desalination. 2014;**347**:175-183. DOI: 10.1016/j.desal.2014.05.015

[37] Choi S-S, Lee YS, Joo CW, Lee SG, Park JK, Han K-S. Electrospun PVDF nanofiber web as polymer electrolyte or separator. Electrochimica Acta. 2004;**50**:339-343. DOI: 10.1016/j.electacta.2004.03.057

[38] Gao K, Hu X, Dai C, Yi T. Crystal structures of electrospun PVDF membranes and its separator application for rechargeable lithium metal cells. Materials Science and Engineering: B. 2006;**131**:100-105. DOI: 10.1016/j.mseb.2006.03.035

[39] Liao Y, Wang R, Tian M, Qiu C, Fane AG. Fabrication of polyvinylidene fluoride (PVDF) nanofiber membranes by electro-spinning for direct contact membrane distillation. Journal of Membrane Science. 2013;**425**:30-39. DOI: 10.1016/j.memsci.2012.09.023

[40] Ding Y, Zhang P, Long Z, Jiang Y, Xu F, Di W. Preparation of PVdF-based electrospun membranes and their application as separators. Science and Technology of Advanced Materials. 2008;**9**:015005. DOI: 10.1088/1468-6996/9/1/015005

[41] Zhao Z, Zheng J, Wang M, Zhang H, Han CC. High performance ultrafiltration membrane based on modified chitosan coating and electrospun nanofibrous PVDF scaffolds. Journal of Membrane Science. 2012;**394**:209-217. DOI: 10.1016/j.memsci.2011.12.043

[42] Liu Z, Pan C, Lin L, Huang J, Ou Z. Direct-write PVDF nonwoven fiber fabric energy harvesters via the hollow cylindrical near-field electrospinning process. Smart Materials and Structures. 2013;**23**:025003. DOI: 10.1088/0964-1726/23/2/025003

[43] Yang Y, Centrone A, Chen L, Simeon F, Hatton TA, Rutledge GC. Highly porous electrospun polyvinylidene fluoride (PVDF)-based carbon fiber. Carbon. 2011;**49**:3395-3403. DOI: 10.1016/j.carbon.2011.04.015

[44] Liu X, Kuang X, Xu S, Wang X. High-sensitivity piezoresponse force microscopy studies of single polyvinylidene fluoride nanofibers. Materials Letters. 2017;**191**:189-192. DOI: 10.1016/j.matlet.2016.12.066

[45] Baji A, Mai Y-W, Li Q, Liu Y. Electrospinning induced ferroelectricity in poly (vinylidene fluoride) fibers. Nanoscale. 2011;**3**:3068-3071. DOI: 10.1039/C1NR10467E

[46] Liu Z, Pan C, Lin L, Lai H. Piezoelectric properties of PVDF/MWCNT nanofiber using near-field electrospinning. Sensors and Actuators A: Physical. 2013;**193**:13-24. DOI: 10.1016/j.sna.2013.01.007

[47] Salimi A, Yousefi A. Analysis method: FTIR studies of β-phase crystal formation in stretched PVDF films. Polymer Testing. 2003;**22**:699-704. DOI: 10.1016/S0142-9418(03)00003-5

[48] Liu X, Deng M, Wang X. Nanoscale domain imaging and local piezoelectric coefficient d 33 studies of single piezoelectric polymeric nanofibers. Materials Letters. 2017;**189**:66-69. DOI: 10.1016/j.matlet.2016.11.044

[49] Song Y, Shen Y, Liu H, Lin Y, Li M, Nan C-W. Enhanced dielectric and ferroelectric properties induced by dopamine-modified $BaTiO_3$ nanofibers in flexible poly (vinylidene fluoride-trifluoroethylene) nanocomposites. Journal of Materials Chemistry. 2012;**22**:8063-8068. DOI: 10.1039/C2JM30297G

[50] Guzhova A, Galikhanov M, Gorokhovatsky YA, Temnov D, Fomicheva E, Karulina E, et al. Improvement of polylactic acid electret properties by addition of fine barium titanate. Journal of Electrostatics. 2016;**79**:1-6. DOI: 10.1016/j.elstat.2015.11.002

[51] Huang Z-X, Liu X, Wu J, Wong S-C, Chase GG, Qu J-P. Electrospun poly (vinylidene fluoride) membranes functioning as static charge storage device with controlled crystalline phase by inclusions of nanoscale graphite platelets. Journal of Materials Science. 2018;**53**:3038-3048. DOI: 10.1007/s10853-017-1723-0

[52] Huang Z-X, Liu X, Zhang X, Wong S-C, Chase GG, Qu J-P, et al. Electrospun polyvinylidene fluoride containing nanoscale graphite platelets as electret membrane and its application in air filtration under extreme environment. Polymer. 2017;**131**:143-150. DOI: 10.1016/j.polymer.2017.10.033

[53] Lee JS, Kim GH, Hong SM, Choi HJ, Seo Y. Surface functionalization of a poly (vinylidene fluoride): Effect on the adhesive and piezoelectric properties. ACS Applied Materials & Interfaces. 2009;**1**:2902-2908. DOI: 10.1021/am900616s

[54] Kim SJ, Raut P, Jana SC, Chase G. Electrostatically active polymer hybrid aerogels for airborne nanoparticle filtration. ACS Applied Materials & Interfaces. 2017;**9**:6401-6410. DOI: 10.1021/acsami.6b14784

[55] Chattopadhyay S, Hatton TA, Rutledge GC. Aerosol filtration using electrospun cellulose acetate fibers. Journal of Materials Science. 2016;**51**:204-217. DOI: 10.1007/s10853-015-9286-4

[56] Yarin A, Kataphinan W, Reneker DH. Branching in electrospinning of nanofibers. Journal of Applied Physics. 2005;**98**:064501. DOI: 10.1063/1.2060928

[57] Kilic A, Shim E, Pourdeyhimi B. Effect of annealing on charging properties of electret fibers. The Journal of The Textile Institute. 2017;**108**:987-991. DOI: 10.1080/00405000.2016.1207269

[58] Pearce GK. UF/MF pre-treatment to RO in seawater and wastewater reuse applications: A comparison of energy costs. Desalination. 2008;**222**:66-73. DOI: 10.1016/j.desal.2007.05.029

[59] Kim SJ, Ko SH, Kang KH, Han J. Direct seawater desalination by ion concentration polarization. Nature Nanotechnology. 2010;**5**:297-301. DOI: 10.1038/nnano.2010.34

[60] Liao Y, Wang R, Fane AG. Engineering superhydrophobic surface on poly (vinylidene fluoride) nanofiber membranes for direct contact membrane distillation. Journal of Membrane Science. 2013;**440**:77-87. DOI: 10.1016/j.memsci.2013.04.006

[61] Alturkmani A. Industrial Wastewater. 2013

[62] Dermentzis K. Removal of nickel from electroplating rinse waters using electrostatic shielding electrodialysis/electrodeionization. Journal of Hazardous Materials. 2010;**173**: 647-652. DOI: 10.1016/j.jhazmat.2009.08.133

[63] Wu N, Wei H, Zhang L. Efficient removal of heavy metal ions with biopolymer template synthesized mesoporous titania beads of hundreds of micrometers size. Environmental Science & Technology. 2011;**46**:419-425. DOI: 10.1021/es202043u

[64] Kurniawan TA, Chan GYS, Lo W-H, Babel S. Physico–chemical treatment techniques for wastewater laden with heavy metals. Chemical Engineering Journal. 2006;**118**:83-98. DOI: 10.1016/j.cej.2006.01.015

[65] Nasreen SAAN, Sundarrajan S, Nizar SAS, Balamurugan R, Ramakrishna S. Advancement in electrospun nanofibrous membranes modification and their application in water treatment. Membranes. 2013;**3**:266-284. DOI: 10.3390/membranes3040266

[66] Tao Y, Ye L, Pan J, Wang Y, Tang B. Removal of Pb (II) from aqueous solution on chitosan/TiO_2 hybrid film. Journal of Hazardous Materials. 2009;**161**:718-722. DOI: 10.1016/j.jhazmat.2008.04.012

[67] Zhou Y-T, Nie H-L, Branford-White C, He Z-Y, Zhu L-M. Removal of Cu^{2+} from aqueous solution by chitosan-coated magnetic nanoparticles modified with α-ketoglutaric acid. Journal of Colloid and Interface Science. 2009;**330**:29-37. DOI: 10.1016/j.jcis.2008.10.026

[68] Bottino A, Capannelli G, Comite A. Preparation and characterization of novel porous PVDF-ZrO_2 composite membranes. Desalination. 2002;**146**:35-40. DOI: 10.1016/S0011-9164(02)00469-1

[69] Liang S, Xiao K, Mo Y, Huang X. A novel ZnO nanoparticle blended polyvinylidene fluoride membrane for anti-irreversible fouling. Journal of Membrane Science. 2012;**394**: 184-192. DOI: 10.1016/j.memsci.2011.12.040

[70] Liu F, Abed MRM, Li K. Preparation and characterization of poly (vinylidene fluoride) (PVDF) based ultrafiltration membranes using nano γ-Al_2O_3. Journal of Membrane Science. 2011;**366**:97-103. DOI: 10.1016/j.memsci.2010.09.044

[71] Du J, Wu L, Tao C, Sun C. Preparation and characterization of Fe_3O_4/PVDF magnetic composite membrane. Acta Physico-Chimica Sinica. 2004;**20**:598-601. DOI: 10.3866/PKU.WHXB20040609

[72] Trigo CEL, Porto AO, De Lima GM. Characterization of CdS nanoparticles in solutions of P (TFE-co-PVDF-co-prop)/N, N-dimethylformamide. European Polymer Journal. 2004;**40**: 2465-2469. DOI: 10.1016/j.eurpolymj.2004.06.027

[73] Hashim NA, Liu Y, Li K. Preparation of PVDF hollow fiber membranes using SiO_2 particles: The effect of acid and alkali treatment on the membrane performances. Industrial & Engineering Chemistry Research. 2011;**50**:3035-3040. DOI: 10.1021/ie102012v

[74] Rahimpour A, Jahanshahi M, Rajaeian B, Rahimnejad M. TiO_2 entrapped nano-composite PVDF/SPES membranes: Preparation, characterization, antifouling and antibacterial properties. Desalination. 2011;**278**:343-353. DOI: 10.1016/j.desal.2011.05.049

[75] Zhang X, Wang Y, Liu Y, Xu J, Han Y, Xu X. Preparation, performances of PVDF/ZnO hybrid membranes and their applications in the removal of copper ions. Applied Surface Science. 2014;**316**:333-340. DOI: 10.1016/j.apsusc.2014.08.004

[76] Song L, Zhao X, Fu J, Wang X, Sheng Y, Liu X. DFT investigation of Ni (II) adsorption onto MA-DTPA/PVDF chelating membrane in the presence of coexistent cations and organic acids. Journal of Hazardous Materials. 2012;**199**:433-439. DOI: 10.1016/j.jhazmat.2011.11.046

[77] Salehi E, Madaeni SS, Heidary F. Dynamic adsorption of Ni (II) and cd (II) ions from water using 8-hydroxyquinoline ligand immobilized PVDF membrane: Isotherms, thermodynamics and kinetics. Separation and Purification Technology. 2012;**94**:1-8. DOI: 10.1016/j.seppur.2012.04.004

[78] WHO—Geneva C. Desalination for Safe Water Supply: Guidance for the Health and Environmental Aspects Applicable to Desalination. Available Online. Geneva, Switzerland: World Health Organization (WHO); 2007

[79] Kaur S, Sundarrajan S, Rana D, Matsuura T, Ramakrishna S. Influence of electrospun fiber size on the separation efficiency of thin film nanofiltration composite membrane. Journal of Membrane Science. 2012;**392**:101-111. DOI: 10.1016/j.memsci.2011.12.005

[80] Wang G, Pan C, Wang L, Dong Q, Yu C, Zhao Z, et al. Activated carbon nanofiber webs made by electrospinning for capacitive deionization. Electrochimica Acta. 2012;**69**:65-70. DOI: 10.1016/j.electacta.2012.02.066

[81] Prince JA, Singh G, Rana D, Matsuura T, Anbharasi V, Shanmugasundaram TS. Preparation and characterization of highly hydrophobic poly (vinylidene fluoride)–clay nanocomposite nanofiber membranes (PVDF–clay NNMs) for desalination using direct contact membrane distillation. Journal of Membrane Science. 2012;**397**:80-86. DOI: 10.1016/j.memsci.2012.01.012

[82] Hoover LA, Schiffman JD, Elimelech M. Nanofibers in thin-film composite membrane support layers: Enabling expanded application of forward and pressure retarded osmosis. Desalination. 2013;**308**:73-81. DOI: 10.1016/j.desal.2012.07.019

[83] Lalia BS, Guillen-Burrieza E, Arafat HA, Hashaikeh R. Fabrication and characterization of polyvinylidenefluoride-co-hexafluoropropylene (PVDF-HFP) electrospun membranes for direct contact membrane distillation. Journal of Membrane Science. 2013;**428**:104-115. DOI: 10.1016/j.memsci.2012.10.061

[84] Mei Y, Yao C, Fan K, Li X. Surface modification of polyacrylonitrile nanofibrous membranes with superior antibacterial and easy-cleaning properties through hydrophilic flexible spacers. Journal of Membrane Science. 2012;**417**:20-27. DOI: 10.1016/j.memsci.2012.06.021

[85] Tijing LD, Woo YC, Johir MAH, Choi J-S, Shon HK. A novel dual-layer bicomponent electrospun nanofibrous membrane for desalination by direct contact membrane distillation. Chemical Engineering Journal. 2014;**256**:155-159. DOI: 10.1016/j.cej.2014.06.076

[86] RE BUXBAUM. Membrane reactor advantages for methanol reforming and similar reactions. Separation Science and Technology. 1999;**34**:2113-2123. DOI: 10.1081/SS-100100759

[87] Cardea S, Reverchon E. Nanostructured PVDF-HFP membranes loaded with catalyst obtained by supercritical CO_2 assisted techniques. Chemical Engineering and Processing: Process Intensification. 2011;**50**:630-636. DOI: 10.1016/j.cep.2011.03.006

[88] Bottino A, Capannelli G, Comite A, Di Felice R. Polymeric and ceramic membranes in three-phase catalytic membrane reactors for the hydrogenation of methylenecyclohexane. Desalination. 2002;**144**:411-416. DOI: 10.1016/S0011-9164(02)00352-1

[89] Samanta S, Nandi AK. Recyclable high performance palladium heterogeneous catalyst with porous PVDF binder from the novel gel nanocomposite route. The Journal of Physical Chemistry C. 2009;**113**:4721-4725. DOI: 10.1021/jp810160r

[90] Gotardo MC, Guedes AA, Schiavon MA, José NM, Yoshida IVP, Assis MD. Polymeric membranes: The role this support plays in the reactivity of the different generations of metalloporphyrins. Journal of Molecular Catalysis A: Chemical. 2005;**229**:137-143. DOI: 10.1016/j.molcata.2004.11.014

[91] Shore SG, Ding E, Park C, Keane MA. Vapor phase hydrogenation of phenol over silica supported Pd and Pd.Yb catalysts. Catalysis Communications. 2002;**3**:77-84. DOI: 10.1016/S1566-7367(02)00052-3

IntechOpen